FINITE ELEMENT MULTISCALE METHODS FOR POISSON'S EQUATION WITH RAPIDLY VARYING HETEROGENEOUS COEFFICIENTS

D. Elfverson[1], A. Målqvist[1]

[1] Department of Scientific Computing, Uppsala University (daniel.elfverson@it.uu.se)

Abstract. *An abstract framework for constructing finite element multiscale methods is presented. Using this framework we propose and compare two different multiscale methods, one based on the continuous Galerkin finite element method and one on the discontinuous Galerkin finite element method. In these multiscale methods the solution is split into coarse and fine scale contributions. The fine scale contribution is obtained by solving localized constituent problems on patches and is used to obtain a modified coarse scale equation. The localized constituent problems are completely parallelizable i.e, no communication between the different problems are needed. The modified coarse scale equation has considerably less degrees of freedom than the original problem. Numerical experiments are presented where the effect of the patch size of the local constituent problems as well as the convergence of the multiscale methods are investigated and compared for the proposed multiscale methods. We conclude that for a given accuracy and a fixed number of patches, smaller patches can be used for the discontinuous Galerkin multiscale method compared to the continuous Galerkin multiscale method.*

Keywords: *finite element methods, discontinuous Galerkin, multiscale methods*

1. INTRODUCTION

There are numerous applications which involves solutions that varies over several different scales, for example flow in porous media such as oil reservoir simulations and CO_2 storage. These, so called multiscale problems, are often impossible to solve with standard single mesh methods since the finest scale needs to be resolved to get a reliable result, see e.g. [5].

To resolve this problem several multiscale methods have been developed during the last two decades e.g., the Multiscale Finite Element Method (MsFEM) by Hou and Wu [9] and the Variational Multiscale Method (VMS) by Hughes [10]. See also [8,7,12] and references therein for recent development and exposition. Using the framework of the Variational Multiscale Methods Larson and Målqvist introduced the Adaptive Variational Multiscale method [11]. This method has further been developed in [12], where the framework for constructing multiscale methods used in this paper is presented and further discussed.

Lately, there have been a lot of interest in discontinuous Galerkin multiscale methods. Discontinuous Galerkin (DG) methods appeared in the 1970s; see [3,6] for some early work for elliptic problem and [4,14,15] for a literature review. A desired property with DG methods is that they admits good conservation properties of the state variable and are ideally suited for application to complex and irregular meshes. Conservation is a crucial property for multiscale problems. Recently proposed multiscale discontinuous Galerkin methods include e.g., [1] based on the MsFEM, and [2] based on the Heterogeneous Multiscale Method.

In this paper a continuous Galerkin multiscale method and a discontinuous Galerkin multiscale method for solving Poisson's equation with rapidly variable heterogeneous coefficients are studied. The continuous Galerkin version was first presented in [11], while the DG version is new. In the proposed multiscale method the solution is split into coarse and fine scale contributions. The fine scale contribution is obtained by solving localized constituent problems on patches and is used to obtain a modified coarse scale equation. Both a symmetric and a non-symmetric version of the modified coarse scale equation are presented. Numerical experiments are presented, where the size needed for the constituent problems to get a sufficient approximation as well as the convergence of the different multiscale methods, are investigated. We conclude that for a given accuracy and a fixed number of patches, smaller patches can be used for the discontinuous Galerkin multiscale compared to the continuous Galerkin multiscale method. On the coarse scale the discontinuous Galerkin multiscale method is approximating the L^2-projection, rather than the nodal values, which is the case for continuous Galerkin multiscale method. The property of approximating the L^2-projection is preferable in a multiscale setting. Also, DG has better conservation properties than CG.

The precise setting of the paper is the following. We consider the following model problem:

$$
\begin{aligned}
-\nabla \cdot \alpha \nabla u = f \quad & u \in \Omega, \\
\mathbf{n} \cdot \nabla u = 0 \quad & u \in \partial\Omega,
\end{aligned}
\tag{1}
$$

where $\Omega \subset \mathbb{R}^d$ for $d = 1, 2, 3$, is a polygonal domain and $\alpha \in L^\infty(\Omega)$, such that $\alpha > \beta > 0$, $\beta \in \mathbb{R}$ has multiscale structure. Equation (1) has a unique solution $u \in H^1(\Omega)$ up to a constant for each $f \in L^2(\Omega)$ provided that $\int_\Omega f\, dx = 0$ is satisfied. Defining the L^2-scalar product as $(\cdot, \cdot)_{L^2(\omega)}$ on a domain $\omega \subseteq \Omega$, the weak formulation of (1) reads: find $u \in \mathcal{V} = H^1$ such that

$$
(\alpha \nabla u, \nabla v)_{L^2(\Omega)} = (f, v)_{L^2(\Omega)}, \quad \forall v \in \mathcal{V}.
\tag{2}
$$

The rest of the paper is organized as follows. In Section 2, we present the different finite element methods needed to construct the multiscale methods. In Section 3 an abstract framework for constructing multiscale methods as well as the specific multiscale methods used in the numerical examples are proposed. Section 4, is devoted to some implementation details. Finally, in Section 5 numerical experiment are presented.

2. FINITE ELEMENT METHODS

Let $\mathcal{K} = \{K\}$ be a shape-regular mesh and let Γ denote the set of all edges (or faces in 3D) of the mesh $\mathcal{K}$. The set Γ is the union of two disjoint subsets $\Gamma = \Gamma^I \cap \Gamma^B$, where Γ^I is the union of the interior edges and Γ^B the union of the boundary edges. Given an interior

edge $e = \partial K^+ \cap \partial K^- \subset \Gamma^I$ for $K^+, K^- \in \mathcal{K}$, denote K^+ the element with the higher index and n as the outward unit normal of K^+ on e. Defining $v^+ := v|_{\partial K^+}$ and $v^- := v|_{\partial K^-}$, we set the average and jump operator as,

$$\{v\} = \frac{1}{2}(v^+ + v^-), \quad [v] = v^+ - v^-, \tag{3}$$

for $e \in \Gamma^I$ and

$$\{v\} = v^+, \quad [v] = v^+, \tag{4}$$

for $e \in \Gamma^B$. Also, for a non negative integer p, we denote by $\mathcal{P}_p(K)$, the set of all polynomials on $\mathcal{K}$ of total degree at most p.

2.1. Continuous Galerkin method

In the continuous Galerkin (CG) finite element discretization we are using a conforming approximation of the test space i.e., $\mathcal{V}_h = \{v \in \mathcal{V} : v|_K \in \mathcal{P}_p(K), \forall K \in \mathcal{K}\} \subset \mathcal{V}$. Given a bilinear form $\mathcal{B}_{cg} : \mathcal{V} \times \mathcal{V} \to \mathbf{R}$ and a linear functional $\mathcal{F}_{cg} : \mathcal{V} \to \mathbf{R}$, the continuous Galerkin method reads: find $u_h \in \mathcal{V}_h$ such that

$$\mathcal{B}_{cg}(u_h, v) := (\alpha \nabla u_h, \nabla v)_{L^2(\Omega)} = (f, v)_{L^2(\Omega)} =: \mathcal{F}_{cg}(v), \quad \forall v \in \mathcal{V}_h. \tag{5}$$

2.2. Discontinuous Galerkin method

In the discontinuous Galerkin method discretization we use a non-conforming approximation i.e., $S_h = \{v \in L^2(\Omega) : v|_K \in \mathcal{P}_r(K), \mathcal{K} \in \mathcal{K}\} \not\subset \mathcal{V}$. The discontinuous Galerkin method reads: find $u_h \in S_h$ such that

$$\mathcal{B}_{dg}(u_h, v) = \mathcal{F}_{dg}(v), \quad \forall v \in S_h, \tag{6}$$

where the bilinear form $\mathcal{B}_{dg} : S_h \times S_h \to \mathbb{R}$ and the linear functional $\mathcal{F}_{dg} : S_h \to \mathbb{R}$ are given by

$$\mathcal{B}_{dg}(v, z) := \sum_{K \in \mathcal{K}} (\alpha \nabla v, \nabla z)_{L^2(K)} - \sum_{e \in \Gamma^I} \Big((n \cdot \{\alpha \nabla v\}, [z])_{L^2(e)} \tag{7}$$
$$+ (n \cdot \{\alpha \nabla z\}, [v])_{L^2(e)} - \frac{\sigma_e}{h_e}([v], [z])_{L^2(e)} \Big),$$
$$\mathcal{F}_{dg}(v) := (f, v)_{L^2(\Omega)}, \tag{8}$$

respectively; here $h_e := \mathrm{diam}(e)$, and $\sigma_e \in \mathbb{R}$ is a positive constant, depending on the variable α, large enough to make the bilinear form (7) coercive with respect to the natural energy norm. We refer, e.g., to [14,4] and references therein for details on the analysis of DG methods for elliptic problems.

3. ABSTRACT MULTISCALE METHOD

In the VMS framework, the fine scale finite element space, $\mathcal{W}_h$, is decoupled into coarse and fine scale contributions $\mathcal{W}_h = \mathcal{W}_c \oplus \mathcal{W}_f$, where $\mathcal{W}_c$ is associated with a coarse

mesh $\mathcal{K}_c$. The split between the coarse and the fine scales is determined by an inclusion operator $\mathcal{I}_c : \mathcal{W}_h \to \mathcal{W}_c$. The coarse and fine scale contributions are defined as, $\mathcal{W}_c := \mathcal{I}_c\mathcal{W}_h$ and $\mathcal{W}_f := (I - \mathcal{I}_c)\mathcal{W} = \{v \in \mathcal{W} : \mathcal{I}_c v = 0\}$. There are several different chooses of $\mathcal{I}_c$ e.g. the L^2-projection onto $\mathcal{W}_c$ or the nodal interpolant onto the coarse mesh. Let $\mathcal{B} : \mathcal{W} \times \mathcal{W} \to \mathbb{R}$ be a bilinear form, we can then define a multiscale map $\mathcal{T} : \mathcal{W}_c \to \mathcal{W}_f$ from the coarse to the fine scale as

$$\mathcal{B}(\mathcal{T}v_c, v_f) = -\mathcal{B}(v_c, v_f) \quad \forall v_c \in \mathcal{W}_c \text{ and } \forall v_f \in \mathcal{W}_f. \tag{9}$$

The reference solution and the test function can be decomposed into a coarse and fine-scale contribution; $u_h = u_c + \mathcal{T}u_c + u_f$, $v = v_c + v_f$ where $u_c, v_c \in \mathcal{W}_c$ and $(\mathcal{T}u_c + u_f), v_f \in \mathcal{W}_f$. The multiscale problem reads: find $u_c \in \mathcal{W}_c$ and $v_f \in \mathcal{W}_f$ such that

$$\mathcal{B}(u_c + \mathcal{T}u_c + u_f, v_c + v_f) = \mathcal{F}(v_c + v_f), \quad \forall v_c \in \mathcal{W}_c \text{ and } \forall v_f \in \mathcal{W}_f. \tag{10}$$

The fine scale component u_f can be computed by letting $v_c = 0$ in (10) and using the multiscale map (9). We arrive to the problem: find $u_f \in \mathcal{W}_f$ such that

$$\mathcal{B}(u_f, v_f) = \mathcal{F}(v_f), \quad \forall v_f \in \mathcal{W}_f. \tag{11}$$

The coarse scale solution is obtained by letting $v_f = 0$ in (10): find $u_c \in \mathcal{W}_c$ such that

$$\mathcal{B}(u_c + \mathcal{T}u_c, v_c) = \mathcal{F}(v_c) - \mathcal{B}(u_f, v_c), \quad \forall v_c \in \mathcal{W}_c. \tag{12}$$

In (12), $\mathcal{T}u_c$ and u_f are unknown and obtained by solving (9) and (11). Note that $\mathcal{B}(u_c + \mathcal{T}u_c, \mathcal{T}v_c) = 0$ and $\mathcal{B}(u_f, \mathcal{T}v_c) = \mathcal{F}(\mathcal{T}v_c)$. Then a symmetric formulation of the coarse scale problem is obtained by considering

$$\mathcal{B}(u_c + \mathcal{T}u_c, v_c + \mathcal{T}v_c) = \mathcal{F}(v_c + \mathcal{T}v_c) - \mathcal{B}(u_f, v_c + \mathcal{T}v_c), \quad \forall v_c \in \mathcal{W}_c. \tag{13}$$

The linear systems (12) and (13) has $\dim(\mathcal{W}_c)$ unknowns, but (9) and (11) are equally hard to solve as the original problem and need to be approximated.

3.1. Localization of the multiscale method

Let $\mathcal{N}$ be the index set of all nodes, $\{x_i\}$, in the mesh $\mathcal{K}_c$. Further, given that the coarse space is spanned by basis functions $\mathcal{W}_c = \text{span}\{\phi_j\}$, let $\mathcal{M}_i$ be the index set of all ϕ_j such that $\phi_j(x_i) = 1$, in the continuous setting $\mathcal{M}_i = \{i\}$ and in the discontinuous case $\mathcal{M}_i$ have several entries. For each basis function ϕ_j we solve: find $\mathcal{T}\phi_j \in \mathcal{W}_f$ such that

$$\mathcal{B}(\mathcal{T}\phi_j, v_f) = -\mathcal{B}(\phi_j, v_f), \quad \forall v_c \in \mathcal{W}_f, \tag{14}$$

where $\phi_j + \mathcal{T}\phi_j$ can be viewed as a modified basis function. Because the fast decay of $\phi_j + \mathcal{T}\phi_j$ away from $\text{supp}(\phi_j)$, see [13] for the conforming case, we can solve (9) on small overlapping patches $\omega_i \subset \Omega$ for each basis function ϕ_j where $j \in \mathcal{M}_i$. Defining $\mathcal{W}_f(\omega_i)$ to be $\mathcal{W}_f$ restricted to the patch ω_i, (9) is transformed to: for each $i \in \mathcal{N}$ and $j \in \mathcal{M}_i$ find $\tilde{\mathcal{T}}\phi_j \in \mathcal{W}_f(\omega_i)$ such that

$$\mathcal{B}(\tilde{\mathcal{T}}\phi_j, v_f) = -\mathcal{B}(\phi_j, v_f), \quad \forall v_f \in \mathcal{W}_f(\omega_i) \tag{15}$$

The term (11) can be handled in i similar fashion by splitting the right hand into local contributions using a partition of unity. The size of the patches is determined by adding a superscript L, ω_i^L, as in Definition 1.

Definition 1 *Let $\{\phi_j : j = 1, \ldots, dim(\mathcal{W}_c)\}$ be the Lagrange basis (continuous or discontinuous) of $\mathcal{W}_c$. The sum $\Phi_i := \sum_{j \in \mathcal{M}_i} \phi_j$ constructs a standard continuous Lagrangian basis function. We say that ω_i^1 is an 1-layer patch, if $\omega_i^1 = supp(\Phi_i)$. Further, we say that ω_i^L is an L-layer patch if*

$$\omega_i^L = \cup_{\{i:supp(\Phi_i) \cap \omega_i^{L-1}\} \neq \varnothing} supp(\Phi_i), \quad L = 2, 3, \ldots . \tag{16}$$

Finally, the set $\omega_i^L \backslash \omega_i^{L-1}$ will be referred to as an L-ring. This is illustrated in Figure 2.
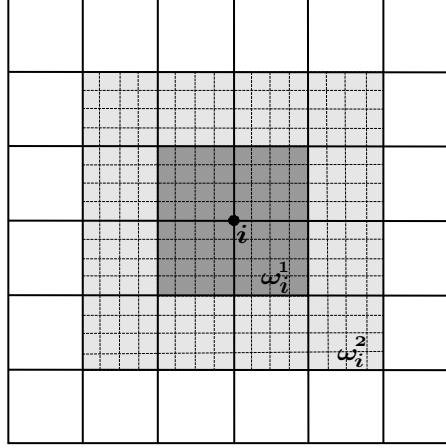

Figure 1. Example of a 1 layer patch ω_i^1 and 2 layer patch ω_i^2 around node i.

3.2. Continuous Galerkin multiscale method

The split between the coarse and fine scale spaces, $\mathcal{V}_h = \mathcal{V}_c \oplus \mathcal{V}_f$, is realized by choosing the inclusion operator to be the nodal interpolant; $\mathcal{I}_c = \Pi_c$. To keep the conformity of the method the fine scale problem is solved on patches using Dirichlet boundary condition. The multiscale problem reads: for all $i \in \mathcal{N}$ find $\tilde{\mathcal{T}} \phi_i, U_{f,i} \in \mathcal{V}_f(\omega_i^L)$ such that

$$
\begin{aligned}
\mathcal{B}_{cg}(\tilde{\mathcal{T}} \phi_j, v) &= -\mathcal{B}_{cg}(\phi_j, v), \quad \forall v_f \in \mathcal{V}_f(\omega_i^L), \\
\mathcal{B}_{cg}(U_{f,i}, v) &= \mathcal{F}_{cg}(\phi_i v), \quad \forall v_f \in \mathcal{V}_f(\omega_i^L).
\end{aligned} \tag{17}
$$

The modified coarse scale equations is then formulated as: find $U_c \in \mathcal{V}_c$ such that

$$\mathcal{B}_{cg}(U_c + \tilde{\mathcal{T}} U_c, v_c) = \mathcal{F}_{cg}(v_c) - \mathcal{B}_{cg}(U_f, v_c), \quad \forall v_c \in \mathcal{V}_c, \tag{18}$$

for the non-symmetric formulation and as

$$\mathcal{B}_{cg}(U_c + \tilde{\mathcal{T}} U_c, v_c + \tilde{\mathcal{T}} v_c) = \mathcal{F}_{cg}(v_c + \tilde{\mathcal{T}} v_c) - \mathcal{B}_{cg}(U_f, v_c + \tilde{\mathcal{T}} v_c), \quad \forall v_c \in \mathcal{V}_c, \tag{19}$$

for the symmetric formulation. The solution to the multiscale problem is $U = U_c + \tilde{\mathcal{T}} U_c + U_f$ where $U_f = \sum_{i \in \mathcal{N}} U_{f,i}$.

3.3. Discontinuous Galerkin multiscale method

Exploiting the discontinuous nature of S_h the split between the coarse and fine spaces, $S_h = S_c \oplus S_f$, is realized by choosing the inclusion operator to be the element wise L^2-projection onto S_c; $\mathcal{I}_c = \mathcal{P}_c$. This is more natural in a multiscale setting since the coarse scale solution approximate the average on each coarse element rather than the nodal values. The discontinuous nature of S_h also allows for using Neumann boundary conditions on the fine scale problems. With $\mathcal{V}_c = \text{span}\{\phi_j\}$, we need to solve the fine scale problem: for all $i \in \mathcal{N}$ and $j \in \mathcal{M}_i$ where $\Phi_i = \sum_{j \in \mathcal{M}_i} \phi_j$ find $\tilde{\mathcal{T}}\phi_j, U_i^f \in S_f(\omega_i^L)$ such that

$$
\begin{aligned}
\mathcal{B}_{dg}(\tilde{\mathcal{T}}\phi_j, v) &= -\mathcal{B}_{dg}(\phi_j, v), \quad \forall v_f \in S_f(\omega_i^L), \\
\mathcal{B}_{dg}(U_i^f, v) &= \mathcal{F}_{dg}(\Phi_i v), \quad \forall v_f \in S_f(\omega_i^L).
\end{aligned}
\tag{20}
$$

The modified coarse scale equations are formulated as: find $U_c \in S_c$ such that

$$
\mathcal{B}_{dg}(U_c + \tilde{\mathcal{T}}U_c, v_c) = \mathcal{F}_{dg}(v_c) - \mathcal{B}_{dg}(U_f, v_c), \quad \forall v_c \in S_c,
\tag{21}
$$

for the non-symmetric formulation or

$$
\mathcal{B}_{dg}(U_c + \tilde{\mathcal{T}}U_c, v_c + \tilde{\mathcal{T}}v_c) = \mathcal{F}_{dg}(v_c + \tilde{\mathcal{T}}v_c) - \mathcal{B}_{dg}(U_f, v_c + \tilde{\mathcal{T}}v_c), \quad \forall v_c \in S_c,
\tag{22}
$$

for the symmetric formulation. The solution to the multiscale problem is $U = U_c + \tilde{\mathcal{T}}U_c + U_f$ where $U_f = \sum_{i \in \mathcal{N}} U_{f,i}$.

4. IMPLEMENTATION

In the proposed multiscale method, the fine scale problem is perfectly parallelizable i.e., no communication between different fine scale problems are required. Algorithm 1 shows how the multiscale methods can be implemented. Note that the outer for-loop is perfectly parallel. An schematic overview is given in Figure 2 where the lines between the boxes represent communication. Also, note that the assembly of the coarse stiffness matrix and load vector is also done in parallel, in the fine scale problems. The extra constraints on the fine scale problems are realized using Lagrange multipliers

---
Algorithm 1 Multiscale Method

1: Initialize the coarse mesh with mesh size H.
2: Let the fine mesh size be $h = H/2^n$ and the size of the patches L.
3: **for** $i \in \mathcal{N}$ **do**
4:     Determine the patch ω_i^L.
5:     **for** $j \in \mathcal{M}_i$ **do**
6:         Compute the fine scale contribution for the modified basis functions $\tilde{\mathcal{T}}\phi_j$.
7:     **end for**
8:     Compute the right hand side correction U_i^f.
9: **end for**
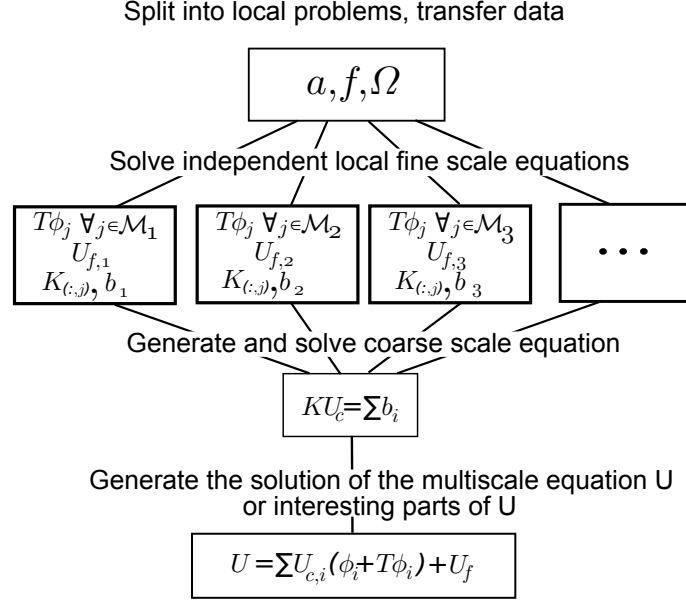10: Solve the modified coarse scale problem to obtain U_c.

Split into local problems, transfer data

$$a, f, \Omega$$

Solve independent local fine scale equations

| $T\phi_j \ \forall_{j \in \mathcal{M}_1}$ $U_{f,1}$ $K_{(:,j)}, b_1$ | $T\phi_j \ \forall_{j \in \mathcal{M}_2}$ $U_{f,2}$ $K_{(:,j)}, b_2$ | $T\phi_j \ \forall_{j \in \mathcal{M}_3}$ $U_{f,3}$ $K_{(:,j)}, b_3$ | $\cdots$ |

Generate and solve coarse scale equation

$$KU_c = \sum b_i$$

Generate the solution of the multiscale equation U
or interesting parts of U

$$U = \sum U_{c,i}(\phi_i + T\phi_i) + U_f$$

Figure 2. Implementation scheme of the discontinuous Galerkin multiscale method.

5. NUMERICAL EXPERIMENTS

5.1. Decay of modified basis functions

Consider the domain ω_i^L, for $L = 1, \dots, N$. On ω_i^N for $N = 8$, let $\mathcal{K}_c$ be a coarse mesh consisting of 16×16 elements and $\mathcal{K}_f$ be a fine mesh consisting of 128×128 elements. Let $\tilde{\mathcal{T}}^L \phi_j \in \mathcal{W}_f(\omega_i^L)$ be the solution of

$$\mathcal{B}(\tilde{\mathcal{T}}^L \phi_j, v) = -\mathcal{B}(\phi_j, v), \quad \forall v \in \mathcal{W}_f(\omega_i^L), \tag{23}$$

computed on ω_i^L and extended by 0 in $\Omega \setminus \omega_i^L$, where $\phi_j \in \mathcal{M}_i$, is a basis function on the coarse scale. Three types of permeabilities, called *Ones*, *Period*, and *SPE*, are used. For *One*, $a = 1$, for *Period*, $\alpha = 1$ or $\alpha = 0.1$ with a period of $1/64$ in x-direction, and *SPE*, data is taken from the 31st layer permeability data in the tenth SPE comparative solution project[1] and illustrated in Figure 3. The aspect ration is $a_{max}/a_{min} = 5.9823 \cdot 10^5$. The decay of the coarse modified basis function $\phi_j + \tilde{\mathcal{T}}^L \phi_j$ is illustrated by computing $\tilde{\mathcal{T}}^L \phi_j$ for $L = 1, \dots, N-1$ using $\tilde{\mathcal{T}}^N \phi_j$ as a reference solution. The space $\mathcal{W}_f$ and the bilinear form $\mathcal{B}(\cdot, \cdot)$, are defined as $\mathcal{V}_f$ and $\mathcal{B}_{cg}(\cdot, \cdot)$ for the continuous Galerkin multiscale method, and as S_f and $\mathcal{B}_{dg}(\cdot, \cdot)$ for the discontinuous Galerkin multiscale method. Exponential decay, in the broken energy norm

$$|||v|||^2 = \sum_{K \in \mathcal{K}_f} \|\sqrt{\alpha} \nabla v\|_{L^2(K)}^2, \tag{24}$$

for $L = 1, \dots, N$ when $N = 4$, is observed in Figure 4. The fast decay motivates us to solve the constituent problems on patches $\omega_i^L \subset \Omega$ using a small number of L-rings. This, in turn, means less computational work and a smaller overlap between the localized problems. The DG method converges faster than CG to to the reference solution in the relative broken energy

---

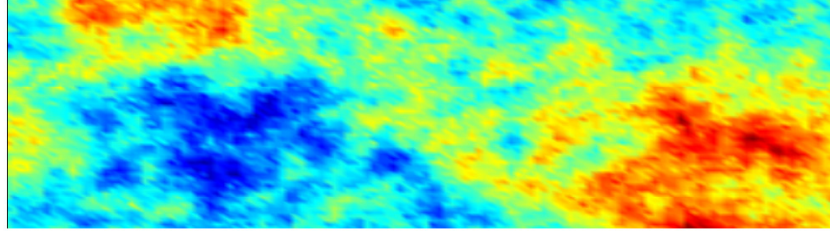[1]Tenth SPE comparative solution project http://www.spe.org/web/csp/

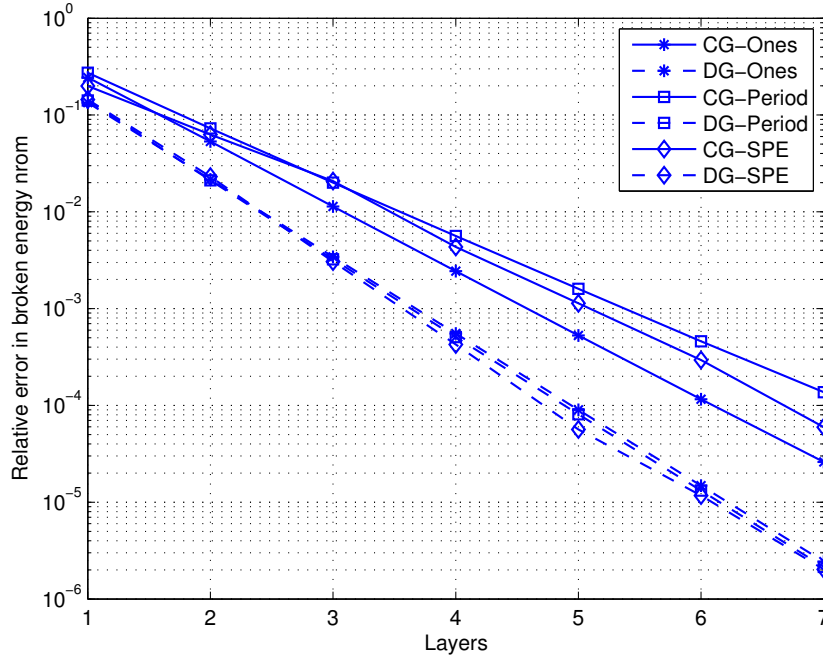Figure 3. Permeability structure for *SPE* (c) in log scale.

Figure 4. Convergence in the relative energy norm (24) when $L = 1, 2, 3$ in equation (23) for different permeability using continuous Galerkin (solid line) and discontinuous Galerkin (dashed line).

norm (24). Hence, smaller patches are needed for solving the local problems using DG than CG to achieve the same accuracy.

5.2. Comparison of the continuous and discontinuous Galerkin multiscale methods

Consider the model problem (1) on the unit square $\Omega = (0, 1) \times (0, 1)$. Let $\mathcal{K}$ be a reference mesh with $MN \times MN$ elements, and $\mathcal{K}_c$ a coarse mesh of $N \times N$ elements i.e., each coarse elements is further subdivided into $M \times M$ elements. In the numerical experiment $N = 16$ and $M = 8$. Let, $f(x, y) = -1$ for $\{0 < x, y < 1/128\}$, $f(x, y) = 1$ for $\{127/128 < x, y < 1\}$, and $f = 0$ otherwise, be the forcing function. The same permeabilities, *Ones*, *Rand* and *SPE*, as in Section 5.1 are used. In the numerical experiments all patches, ω_i^L, are of the same size, L, and for each iteration L is increased by one. The continuous Galerkin multiscale method and the discontinuous Galerkin multiscale method are compared, see Figure 5. We conclude:
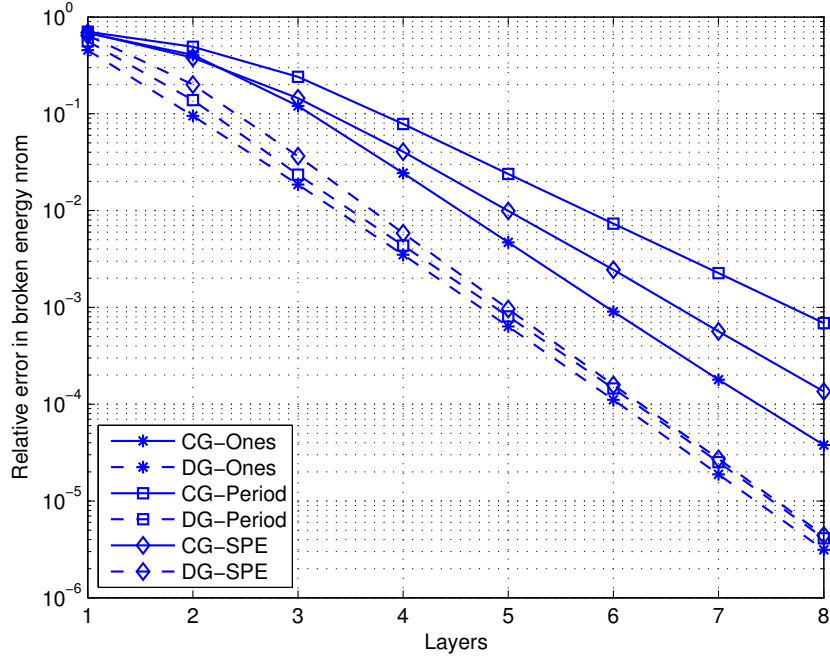
Figure 5. Convergence in the broken relative energy norm (24) when $L = 1, 2, \ldots, 8$ for different permeability using continuous Galerkin multiscale method (solid line) and discontinuous Galerkin multiscale method (dashed line).

- To obtain a given accuracy, in the relative broken energy norm (24), the discontinuous Galerkin multiscale method requires approximately one layer less than the continuous Galerkin multiscale method. For a comparison of the degrees of freedom required for the fine scale problems, see Table 1.

- This is a bit unfair comparison since the reference solution is the DG respectively CG solution computed on the fine scale. DG has a more enriched test and trial space and may give a better approximation than CG because of the discontinuous permeability coefficients.

- On the coarse scale the discontinuous Galerkin multiscale method is approximating the L^2-projection rather than the nodal values, which is the case for continuous Galerkin multiscale method. This is preferable in a multiscale setting.

- The DG method has better conservation properties which is an important property in many multiscale applications.

Table 1. Degree of freedom for the fine scale problems

layers	CGMM	DGMM
1	$(2n + 1)^d$	$(4n)^d$
2	$(4n + 1)^d$	$(8n)^d$
3	$(6n + 1)^d$	$(12n)^d$
4	$(8n + 1)^d$	$(16n)^d$

6. REFERENCES

[1] J. Aarnes, B.-0. Hemsund, "Multiscale discontinuous Galerkin methods for elliptic problems with multiple scale". *Letc. notes in Comput. Sci. Eng.* vol 44, Springer, Heidelberg, Berlin, 2005.

[2] A. Abdulle, "Discontinuous Galerkin finite element heterogeneous multiscale method for elliptic problems with multiple scale". *Math. Comp.* 81, 687-713, 2012.

[3] D. N. Arnold, "An interior penalty finite element method with discontinuous elements". *SIAM J. Numer. Anal.* 19, 742-760, 1982.

[4] D. N. Arnold, F. Brezzi, B. Cockburn, L. Marini "Unified analysis of discontinuous Galerkin methods for elliptic problems". *SIAM J. Numer. Anal.* 39, 1749-1779, 2001.

[5] A. Babuška, J. E. Osborn, "Can a finite element method perform arbitrarily bad?". *Math. Comp.* 69(230), 443-462, 2000.

[6] G. A. Baker, "Finite element methods for elliptic equations using nonconforming elements". *Math. Comp* 31, 45-59, 1977.

[7] W. E, "Principles of multiscale modeling". *Math. Model. and Methods* Cambridge university press, 2011.

[8] Y. Efendiev, T. Y. Hou, "Multiscale finite element methods: Theory and Applications". *Surveys and Tut. in Appl. Math. Sci.*, vol 4, Springer, New York,2009

[9] T. Y. Hou, X.-H. Wu, "A multiscale finite element method for elliptic problems in composite materials and porous media". *J. of Comput. Phys.* 134, 169-189, 1997

[10] T. Hughes, "Multiscale phenomena: Green's functions, the Dirichlet-to-Neumann formulation, subgrid scale models, bubbles and the origins of stabilized methods". *Comput. Methods Appl. Mech. Engrg.* 166(1-2), 3-24, 1998.

[11] M. G. Larson, A. Målqvist, "Adaptive variational multiscale methods based on a posteriori error estimation: Energy norm estimates for elliptic problems". *Comput. Mehtods Appl. Mech. Engrg. s* 196(21-24), 2313-2324, 2007.

[12] A. Målqvist, "Multiscale methods for elliptic problems". *Multiscale Model. and Simul.* 9, 1064-1086, 2011.

[13] A. Målqvist, D. Perterseim "Localization of elliptic multiscale problems". *arXiv:1110.0692.* Submitted, 2011.

[14] D. A. Di Pietro, A. Ern, "Mathematical aspect of discontinuous Galerkin methods". *Mathématiques et Apllications* vol 19, Springer, 2012.

[15] B. Rivière, "Discontinuous Galerkin methods for solving elliptic and parabolic equations: Theory and Implementation". *Soc. for Industrial and Applied Math.*, Philadelphia, PA, USA. 2008